Molecular Diagnosis in Ewing Family Tumors

The Rizzoli Experience—222 Consecutive Cases in Four Years

Gabriella Gamberi,* Stefania Cocchi,*
Stefania Benini,* Giovanna Magagnoli,*
Luca Morandi,[†] Jennifer Kreshak,*
Marco Gambarotti,* Piero Picci,* Licciana Zanella,*
and Marco Alberghini*

From the Department of Pathology, Rizzoli Institute, Bologna;
and the Department of Hematology and Oncological Sciences
Section of Pathology,[†] Bellaria Hospital, University of
Bologna, Italy*

The Ewing's family of tumors (EFTs) are characterized by chimeric transcripts generated by specific chromosomal rearrangements. The most common fusions are between the *EWSR1* gene on chromosome 22 and the ETS family of transcription factors; rarely, *FUS* (on chromosome 16) substitutes for *EWSR1*. The detection of specific translocations using molecular analysis is now a routine part of the pathological examination of EFT. Here, we report our experience with molecular diagnosis of EFT during the 4 years (2006–2009) at the Rizzoli Institute. We analyzed 222 consecutive tumors with a presumptive diagnosis of EFT using molecular techniques and IHC. We found five distinct types of *EWSR1-FLI1* fusion transcripts resulting from translocation t(11;22), three types of *EWSR1-ERG* transcripts resulting from t(21;22), and one type of t(2;22) resulting in *EWSR1-FEV* fusion. Molecular investigation validated 92% of cases ultimately diagnosed as EFT; IHC validated 76% of the cases. Thus, despite the difficulties and limitations associated with both molecular and IHC analysis on fresh and formalin-fixed, paraffin-embedded tissue, a combination of these techniques is the best approach to enhancing the accuracy of EFT diagnosis. We also present our method for choosing which molecular techniques to apply. Finally, we collected the most prevalent breakpoints reported in the literature, indicating which exons are involved, the sequence breakpoints, and the NCBI reference sequences.   (J Mol Diagn 2011, 13:313–324; DOI: 10.1016/j.jmoldx.2011.01.004)

Ewing's sarcoma (ES) is a highly malignant small round cell tumor (SRCT) that can arise in both bone and soft tissues of children and young adults. Rarely, it occurs also in adults.[1,2] It is the second most common pediatric bone tumor after osteosarcoma, accounting for ~30% of all primary bone tumors in this age group.[1,3,4] Based on their shared immunophenotypes and molecular parameters, several diagnostic entities that were previously considered distinct are now assembled as a single entity, the Ewing's sarcoma family of tumors (EFTs). These include bone and extraskeletal Ewing's sarcoma, primitive neuroectodermal tumor (PNET), and Askin tumor of the thoracopulmonary region.[1,5–7]

The histological evaluation of EFT is based on morphological, immunophenotypic, and molecular features. The morphology of ES is variable. These tumors are frequently composed of uniform small round cells with round nuclei containing fine chromatin, scanty clear or eosinophilic cytoplasm, and indistinct cytoplasmic membranes. In less differentiated cases, tumor cells are larger, with prominent nucleoli and irregular contours. The cytoplasm frequently contains PAS-positive diastase-resistant glycogen. PNET is characterized by Homer-Wright rosettes, which are typical of neuroectodermic differentiation.[6,8,9]

Immunohistochemical analysis (IHC), the first ancillary technique used in pathology to confirm the diagnosis of EFT, can distinguish among different variants. The immunohistochemical features of ES are positivity for CD99, FLI1, and caveolin 1 antigens, whereas PNET also shows immunoreactivity for S100 protein, chromogranin, and synaptophysin antigens. These positive reactions, along with negative reactions for a panel of other markers (including muscular and lymphoid markers), support the diagnosis of EFT.[9]

The EFTs are characterized genetically by specific chromosomal translocations resulting in a fusion of the *EWSR1* (22q12) gene with one of the members of the ETS family of transcription factors: the *FLI1* gene (11q24) in 85% of cases and the *ERG* gene (21q22) in 5%–10% of cases. Less frequently, *EWSR1* is fused with *FEV* (2q36), *ETV1* (7p21), or *ETV4* (alias *E1AF;* 17q21).[4,10–14] There are also rare variants involving the *FUS* (16p11) gene juxtaposed to the *ERG* (21q22) gene, a t(16;21) rear-

rangement.[14,15] In addition, the *FUS-FEV* fusion gene has been described, resulting from the t(2;16)(q36;p11) rearrangement.[16] Finally, two new translocations were recently identified: t(20;22), involving *EWSR1* and *NFATC2* (20q13), and t(4;22), involving *EWSR1* and *SMARCA5* (4q31).[17,18]

Establishing the correct diagnosis of EFT (as opposed to other small round cell tumors) has particular clinical relevance.[19,20] The diagnosis is based on the evaluation of clinical, radiological, and pathological features. The determination of a chimeric transcript by RT-PCR and/or the gene rearrangement involved in a translocation by fluorescence *in situ* hybridization (FISH) is often required for validation of the diagnosis.[21,22]

In the present study, we analyzed 222 tumors with a presumptive diagnosis of EFT. We characterized the fusion transcripts and the gene rearrangement using RT-PCR and FISH, and compared the utility of the different ancillary techniques used to support a diagnosis of EFT. We also reviewed the literature to summarize the most frequent breakpoints found to date.

Materials and Methods

We evaluated 222 consecutive patients with a presumptive diagnosis of EFT who underwent surgery during a 4-year period (2006–2009). The majority of the cases were tumors biopsied or excised at our hospital and processed locally; 61 cases were consultations from outside institutions, sent to us for a second diagnostic opinion.

Of the 222 patients, 149 were male and 73 were female. For each case, either the biopsy specimen or the surgical specimen was analyzed. Part of each sample was used for histological and immunohistochemical characterization, and another portion was frozen for molecular analysis. When frozen tissue was not available or if the amount was too small (eg, from consultations or fine-needle aspiration biopsies), the molecular analysis was performed on formalin-fixed paraffin-embedded (FFPE) tissue.

In our laboratory, the protocol for molecular analysis was determined as follows. Fresh tissue or FFPE tissue was first analyzed by RT-PCR. FISH analysis was used if the material was inadequate for RT-PCR [ie, <1000 tumor cells, poor RNA quality (A260/280 < 1.6)] or if the RT-PCR results were negative (Figure 1). To evaluate fresh tissue tumor cellularity under light microscopy, frozen sections were stained with hematoxylin-eosin. Regarding FFPE tissue, >1000 tumors cells corresponds to a tissue section area of approximately 1–2 mm². In our experience, <1000 tumor cells (eg, in small samples such as from fine-needle aspiration biopsies) is too little for RT-PCR analysis, but is suitable and adequate for a good FISH analysis, for which a minimum of 100 tumor cell nuclei with intact morphology are necessary.
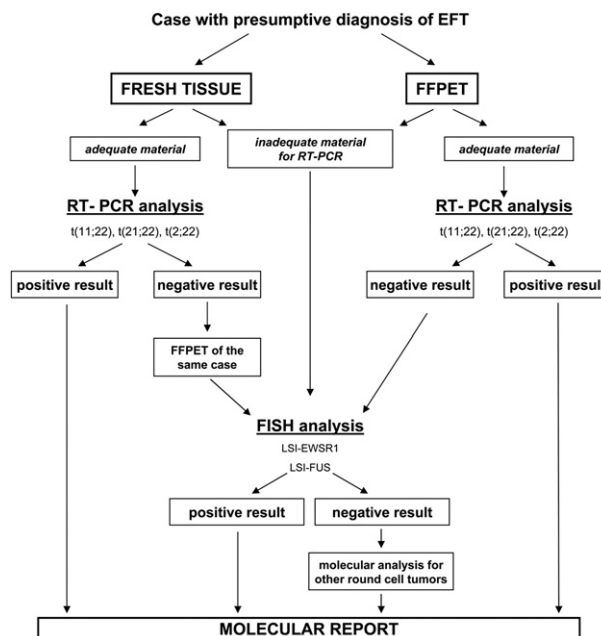

Figure 1. Algorithm showing the protocol used in our laboratory to evaluate the presence of gene rearrangements in tumors with presumptive diagnosis of EFT. FISH, fluorescence *in situ* hybridization; LSI, locus-specific identifier (probe); FFPET, formalin-fixed paraffin-embedded tissue.

RT-PCR

RNA was extracted from fresh tissue using a modified method including TRIzol reagent (Invitrogen, Carlsbad, CA) and the column of an RNeasy mini kit (Qiagen, Hilden Germany; Valencia, CA). To extract RNA from FFPE tissue, sections 6–8 μm in thickness were cut from the representative paraffin block, deparaffinized with xylene, rinsed in ethanol, and digested by proteinase K. The extraction was performed using a Pinpoint slide RNA isolation System II kit (Zymo Research, Glasgow, Scotland, UK). Special attention was paid to the cutting step, and the blade was changed for each paraffin block to avoid any potential contamination.

Further quantification of RNA was done spectrophotometrically by measuring the absorbance at 260 nm (1 optical density unit = 40 μg/mL of RNA). The purity of RNA was determined by the ratio of its readings at 260 and 280 nm (A260/A280); a ratio of >1.6 was considered acceptable.

The RNA (2 μg) was then reverse-transcribed to cDNA using a high-capacity cDNA archive kit (Applied Biosystems, Foster City, CA). The PCR was performed in a total volume of 25 μL; each reaction mixture contained 2.5 μL of 10× PCR buffer (Invitrogen), 1.2 mmol/L magnesium chloride, 0.2 mmol/L of each deoxynucleotide triphosphate, 0.4 mmol/L of each sense and antisense primer, 0.5 U of Taq DNA polymerase (Invitrogen), and 3 μL of the cDNA template.

PCR was performed for detection of the t(11;22) *EWSR1-FLI1*, t(21;22) *EWSR1-ERG*, and t(2;22) *EWSR1-FEV* translocations. The primers used for PCR amplification of EFT translocations are listed in Table 1, rows 1–6) and have been previously reported.[3,11,21,23–26] On fresh

Table 1. Primer Sequences for Fusion Transcripts in Small Round Cell Tumors

	Tumor	Primer	Sequence
1	EFT	F-EWS 22ex7	5'-TCCTACAGCCAAGCTCCAAGTC-3'
2	EFT	R-FLI1 11ex9	5'-ACTCCCCGTTGGTCCCCTCC-3'
3	EFT	R-PARA FLI1	5'-GGACTTTTGTTGAGGCCAGA-3'
4	EFT	R-ERG Q	5'-GGTTGAGCAGCTTTCGACTG-3'
5	EFT	R-FEV 2ex3	5'-TAGCGCTTGCCATGCACCTT-3'
6	EFT	R-FEV F1	5'-GCTTGAACTCGCCGTGACCG-3'
7	EFT	F-EWSB	5'-ACCCACCCCAAACTGGATCC-3'
8	EFT	F-ERGB	5'-CGAACTTGTAGGCGTAGCGC-3'
9	SS	F-SYT	5'-GGACAAGGTCAGCAGTATGGA-3'
10	SS	R-SSX1	5'-TTGGGTCCAGATCTCTTATT-3'
11	SS	R-SSX2	5'-TTGGGTCCAGATCTCTCGTA-3'
12	ARMS	F-PAX3	5'-GCACTGTACACCAAAGCACG-3'
13	ARMS	F-PAX7	5'-CCGACACCAGCTCTGCCTAC-3'
14	ARMS	R-FKHR	5'-ATGAACTTGCTGTGTAGGGACAG-3'
15	IFS	F-ETV6 (TEL 971)	5'-ACCACATCATGGTCTCTGTCTCC-3'
16	IFS	R-NTRK3 1838	5'-CCGCACACTCCATAGAACTTGAC-3'
17	DSRCT	F-EWS 22ex7	5'-TCCTACAGCCAAGCTCCAAGTC-3'
18	DSRCT	R-WT1 ex8	5'-ACCTTCGTTCACAGTCCTTTG-3'
19	MLS	F-FUS ex5	5'-CAGCCAGCAGCCTAGCTATG-3'
20	MLS	F-EWS ex7	5'-CTGGATCCTACAGCCAAGCTCCAAG-3'
21	MLS	R-CHOP ex3	5'-TGTCCCGAAGGAGAAAGGCAATG-3'

ARMS, alveolar rhabdomyosarcomas; DSRCT, desmoplastic small round cell tumor; EFT, Ewing's sarcoma family tumors; ex, exon; IFS, infantile fibrosarcoma; MLS, myxoid liposarcoma; SS, synovial sarcoma. *CHOP* is an alias of *DDIT3*; *FKHR* is a previous gene symbol for *FOXO1*; *SYT* is an alias of *SS18*.

tissue, we used the EWS 22ex7-FLI1 11ex9 primers to evaluate t(11;22), and to evaluate t(21;22) we used primers EWSB-ERGB, designed for us with Primer Express Software version 2.0 (Applied Biosystems). To our knowledge, the primer pair EWSB-ERGB has not been used in previous studies (Table 1, rows 7 and 8). On RNA extracted from FFPE tissue, we were able to obtain satisfactory PCR fragments with PCR primers that generate relatively small PCR products (<250 bp). To evaluate t(11;22), we used the EWS 22ex7-PARA FLI1 primers to detect type 1 (129 bp) and type 2 (195 bp), and to evaluate t(21;22) on FFPE tissue we used the EWS 22ex7-ERG Q primers to detect type 1 (137 bp). The primer pair EWS 22ex7-FEV 2ex3 was used for the detection of t(2;22) on fresh tissue; on FFPE tissue, the EWS 22ex7-FEV F1 primer pair was used to detect t(2;22) type 1 (235 bp). When indicated, we performed RT-PCR for diagnostic exclusion of other small round cell tumors using the previously reported primers listed in Table 1 (rows 9–20),[27–31] according to the pathologist's request.

RNA integrity was assessed with primers for the housekeeping gene β-actin. Positive case controls consisted of a Ewing's sarcoma, which was analyzed by sequencing to confirm the specific translocation. We used the positive controls of the types previously identified in our laboratory. For t(11;22) *EWSR1-FLI1*, we have type 1 (exon 7/6 fusion), type 2 (exon 7/5 fusion), type 3 (exon 10/6 fusion), type 4 (exon 10/5 fusion), type 8 (exon 7/8 fusion), and exon 7/7 fusion positive controls. For t(21;22), we have type 1 (exon 7/6 fusion) positive control, exon 7/10 fusion positive control, and the controls corresponding to EWS-ERG exon 7/13 fusion and EWS-ERG exon 10/10 fusion. For t(2;22), we have the positive control corresponding to *EWSR1-FEV* exon 7/2 fusion. In addition, negative controls (RNA from normal tissue or from other

types of tumors and a water blank) were included in each RT-PCR reaction.

PCR Products

The PCR products were resolved on 2% agarose gel electrophoresis, followed by Gel Star (Lonza, Rockland, ME) staining. The RT-PCR assay was considered suitable for interpretation when the β-actin control product was present, when the positive control for the fusion gene was positive, and when the negative and water controls showed no amplified product (Figure 2).
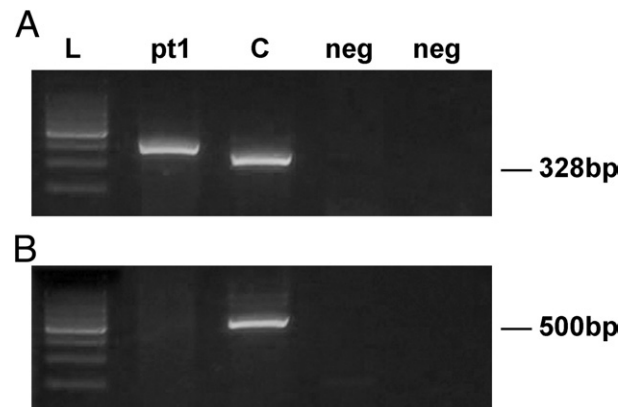

Figure 2. RT-PCR for detection of *EWSR1-FLI1* transcript (**A**) and *EWSR1-ERG* transcript (**B**) in the same patient. **Lane pt1** is the RT-PCR product obtained from patient's tumor RNA. In **A**, the band corresponds to a type 2 *EWSR1-FLI1* fusion transcript; in **B**, no band is present, denoting a negative result for the *EWSR1-ERG* fusion. **Lane C** is the t(11;22) positive control; the band represents type 1 fusion. Lanes marked **neg** are negative controls, and the size marker (**lane L**) is a 100-bp DNA ladder (Promega).
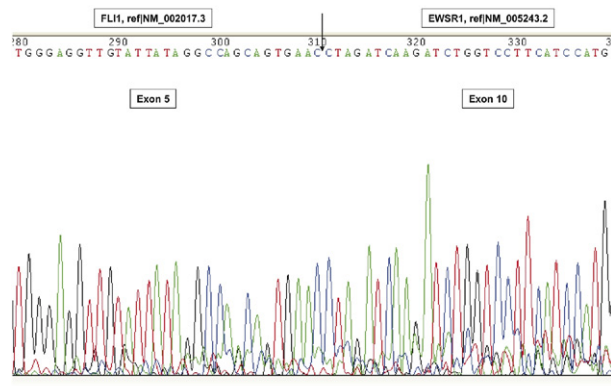
Figure 3. Sequence analysis of an *EWSR1-FLI1* fusion transcript at the breakpoint region, confirming the fusion of *EWSR1* exon 10 to *FLI1* exon 5 resulting in t(11;22) type 4.

Sequencing of RT-PCR Products

The cases in which an unexpected band size was detected were analyzed by automatic sequencing (Figure 3). The sequencing allowed us to typify new types, which were used as positive controls in further analyses. PCR products were separated by electrophoresis on 2% agarose gel and were purified using an Agencourt AMPure magnetic beads kit (Beckman Coulter, Fullerton, CA). Sequencing analysis was then performed on a CEQ2000 XL automatic DNA sequencer (Beckman Coulter). The strands were screened using the same PCR forward and reverse primers as previously described.

The sequencing of some cases was performed by Bio-Fab Research (Rome, Italy), because the number of samples we needed to process was too great for us to process alone.

Computer analysis of sequences was conducted with Basic Local Alignment Search Tool (BLAST) sequence similarity searches using the National Center of Biotechnology Information Database, NCBI (*http://www.ncbi.nlm. nih.gov/BLAST*, last accessed June 17, 2009).

FISH

FISH was performed using Vysis LSI (locus-specific identifier) dual-color, break-apart DNA probes (Abbott Molecular, Des Plaines, IL) for *EWSR1* (22q12) and *FUS* (16p11) according to the manufacturer's protocol. Tissue sections (4 μm thick) were mounted on positively charged slides (Dako, Glostrup, Denmark), a hematoxylin-stained section from each tumor was prepared, and areas of representative non-necrotic neoplasm were marked. Slides were heated overnight (60°C), dewaxed in xylene, and treated with a graded ethanol-to-water series. This was followed by incubation in TE solution (Tris/l-EDTA, 5 mmol/L:1 mmol/L) at 96°C for 15 minutes, then a rinse in distilled water, and digestion with pepsin (0.04%) in 0.01N HCl at 37°C for 5 to 15 minutes, then a wash again in distilled water.

Slides were finally dehydrated in ethanol (96%) and air-dried. Next, the LSI probe was applied to the target

area and the slides were coverslipped and sealed with rubber cement.

The samples and probe were co-denatured in Dako Hybridizer (Dako, Glostrup, Denmark) at 85°C for 1 minute and incubated overnight at 37°C.

The following day, the coverslips were removed and the slides were washed for 2 minutes at 75 ± 1°C in 0.4× standard saline citrate/0.3% NP40 and for 1 minute at room temperature in 2× standard saline citrate/0.1% NP40. The slides were then left to dry in the dark at room temperature; the nuclei were subsequently counterstained in Vectashield antifade solution with DAPI (Vector Laboratories, Burlingame CA).

Fluorescence signals were counted using an Olympus BX41 fluorescence microscope (Olympus, Hamburg Germany), at ×100 magnification under oil immersion using an appropriate filter set. Representative cells were captured using a Color View III CCD camera interfaced with the Soft Imaging System Cell[P] software package version 2.2 (Olympus).

A minimum of 100 tumor cell nuclei with intact morphology as determined by DAPI counterstaining were counted in the previously marked neoplastic area. Cells with nuclear overlap and indistinguishable separate nuclei were excluded from analysis. In normal cells without a translocation, two fused or very close red-green signals were observed (Figure 4A). A positive result was defined as the presence of a visible
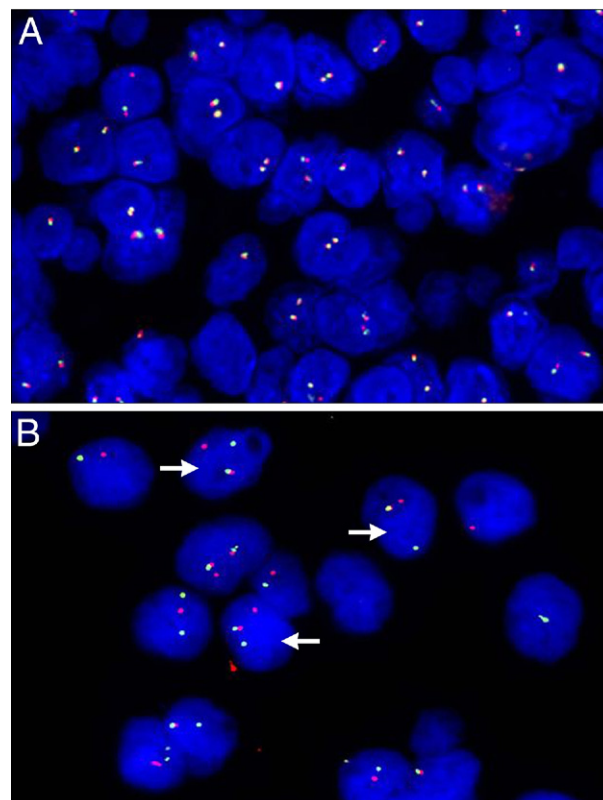

Figure 4. A: Negative FISH analysis of *FUS* showing two normal fusion signals. **B:** Positive FISH analysis of *EWSR1* for the same patient; **arrows** indicate the normal fusion signal and split red and green signals, indicating a rearrangement of one copy of the *EWSR1* region.

Table 2. Antibodies for Immunohistochemical Analysis

Antibody	Clone	Source	Dilution	Pretreatment	Distribution
CD99	12E7	Dako	1:200	None	membranous and cytoplasmic
FLI1	G146-222	Becton Dickinson	1:100	Citrate buffer pH 8.0/95°C/30 minutes	Nuclear
Caveolin 1	N-20	Santa Cruz Biotechnology	1:300	Citrate buffer pH 8.0/95°C/30 minutes	Cytoplasmic
S100	Polyclonal	Dako	1:5000	Proteinase K	Nuclear and cytoplasmic
Terminal deoxynucleotidyl transferase	Polyclonal	Dako	1:40	Citrate buffer pH 8.0/95°C/30 minutes	Nuclear
Leukocyte common antigen	CD45	Dako	Prediluted	None	Cytoplasmic
Epithelial membrane antigen	E-29	Dako	Prediluted	None	Cytoplasmic
Cytokeratin	MNF-116	Dako	1:1200	Proteinase K	Cytoplasmic
Chromogranin A	Polyclonal	Dako	Prediluted	None	Cytoplasmic
Synaptophysin	Polyclonal	Dako	Prediluted	None	Cytoplasmic
Desmin	D-33	Dako	Prediluted	None	Cytoplasmic
Muscle actin	HHF-35	Dako	Prediluted	None	Cytoplasmic
Smooth muscle actin	1A4	Dako	Prediluted	None	Cytoplasmic
Myogenic factor 4 (MYF4)	LO-26	Dako	1:40	Citrate buffer pH 8.0/95°C/30 minutes	Nuclear
Myogenin	F5D	Dako	1:40	Citrate buffer pH 8.0/95°C/30 minutes	Nuclear

translocation (separation of red and green signals >3 signal diameters) in >10% of the cells (Figure 4B). In cells with a translocation involving *EWSR1*, different types of signal patterns were observed in accordance with previous report.[22]

Immunohistochemistry

IHC was performed in all of the cases studied. Formalin-fixed, paraffin-embedded sections, 4 μm thick, were immunostained using an automated immunostainer (Dako,
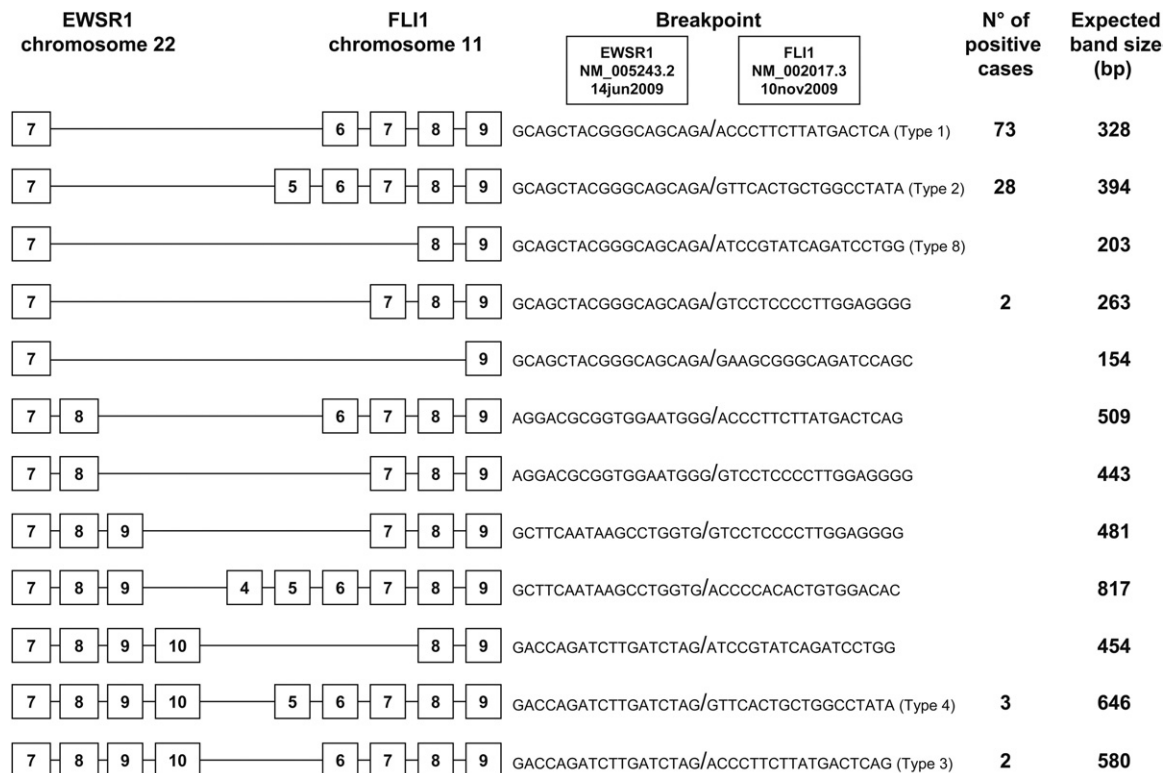

Figure 5. The most prevalent types of exon breakpoints (indicated by **boxed** numbers) for the t(11;22) *EWSR1-FLI1* translocation in EFT, with the number of positive cases identified in our series and the expected band size of the products, using primer pair EWS 22ex7-FLI1 11ex9.
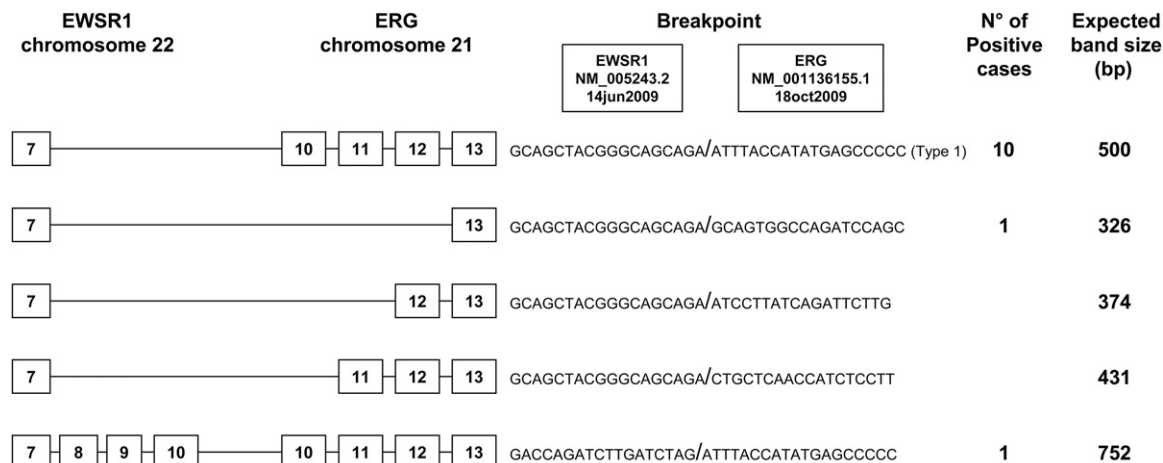
Figure 6. The most prevalent types of exon breakpoints (indicated by **boxed** numbers) for the t(21;22) *EWSR1-ERG* translocation in EFT, with the number of positive cases identified in our series and the expected band size of the products, using primer pair EWSB-ERGB.

Glostrup, Denmark). The various antibodies used are listed in Table 2. The CD99 antibody was used in all cases; the other antibodies were used according to the pathologist's request.

The slides were deparaffined in xylene and then rehydrated in graded alcohols and water. If necessary, endogenous tissue peroxidase was blocked by treating the sections with 0.3% H_2O_2; if necessary, a pretreatment was applied. To reduce nonspecific binding, sections were incubated with normal serum.

Antibody detection was performed using a Dako REAL detection system: streptavidin-biotin alkaline phosphatase/red, rabbit-mouse for cytoplasmic antigens and peroxidase/DAB, rabbit-mouse for nuclear antigens. The slides were stained with hematoxylin and then rehydrated and coverslipped. Appropriate positive and negative controls were included in each run.

In the cases in which histopathological and immunohistochemical features were not suggestive of EFT, nor of SRCT, the IHC analysis of specific markers of other round cell tumors was performed based on differential diagnosis and following the requirements of the pathologist (Table 2).

Results

Many authors have reported sequences that result from the linkage of the *EWSR1* gene to the *FLI1*, *ERG*,
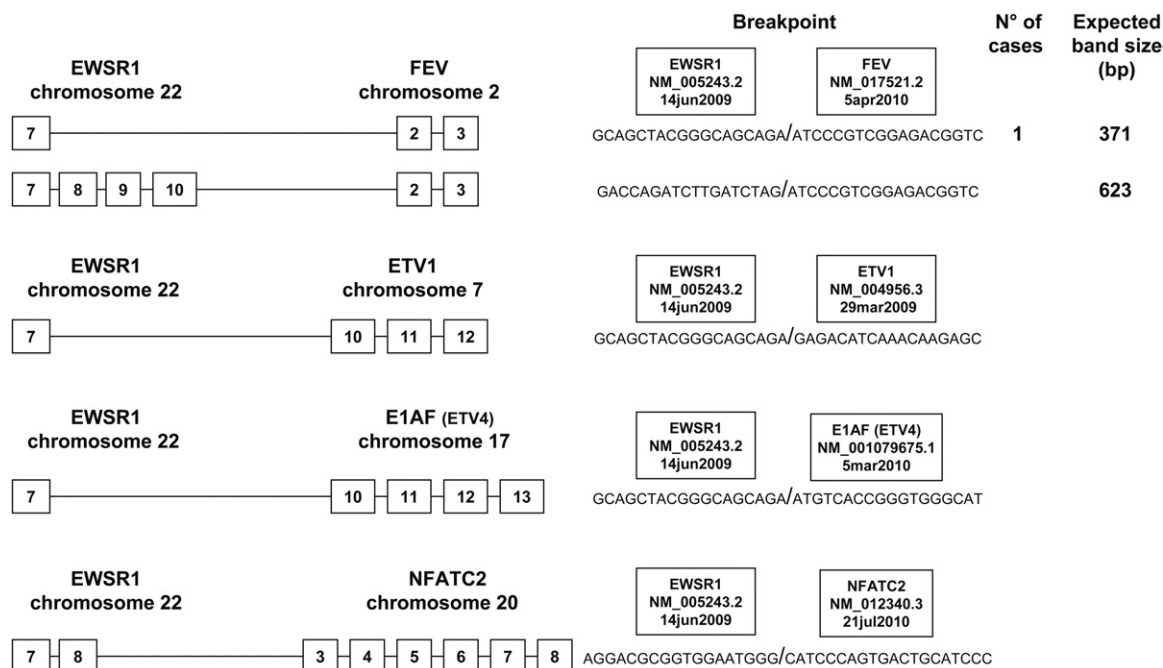

Figure 7. The most prevalent types of exon breakpoints (indicated by **boxed** numbers) for the rare translocations of EFT, with the expected band size of the products, using primer pair EWS 22ex7-FEV 2ex3. In the present study, we detected 1 case with t(2;22) *EWSR1-FEV* translocation. Translocations t(7;22), t(17;22), and t(20;22) are not yet routinely assessed in our laboratory.
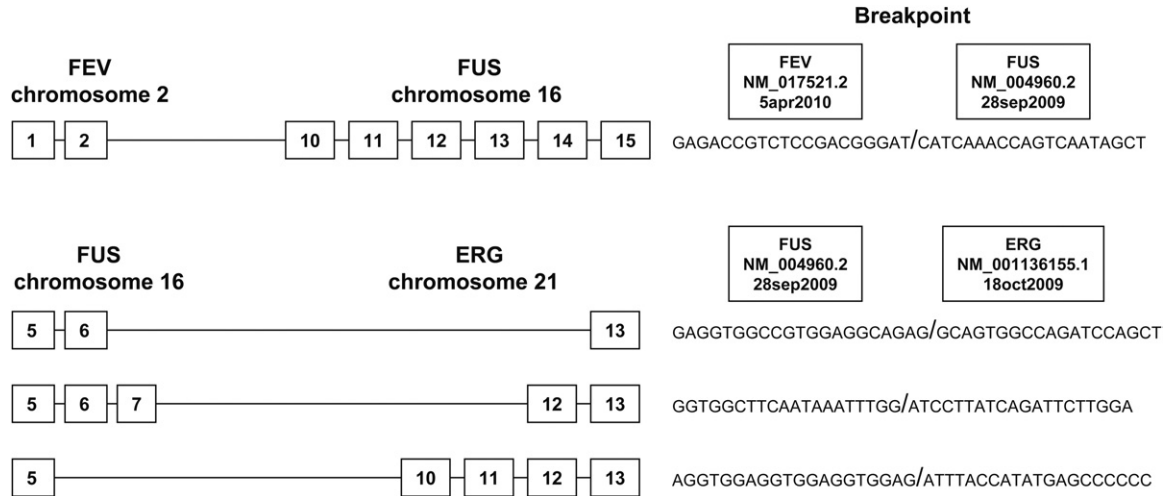
Breakpoint

Figure 8. The types of exon breakpoints (indicated by **boxed** numbers) of the rare variants in which the gene *FUS* is involved. The translocations t(2;16) and t(16;21) are not yet routinely assessed in our laboratory.

FEV, *ETV1*, *ETV4* (alias *E1AF*), and *NFATC2* genes*, as well as those involving the *FUS* gene in Ewing's sarcoma.[14–17,23,25,26,32–35] In Figures 5, 6, 7, and 8, we summarize the most prevalent types of exon fusion described in the literature to date and indicate the sequence breakpoint and the NCBI reference sequences. To our knowledge, the present report is the first to present a single summary of all the most prevalent breakpoint sequences of EFTs.

Of the 222 total cases analyzed, 188 cases (85%) had interpretable results by FISH or RT-PCR (or both techniques) and were thus considered informative from a molecular point of view. For the remaining 34 cases (15%), the molecular results were considered noninformative; these were samples without adequate FISH results (absent and/or weak fluorescence signal) and without acceptable RT-PCR results (absence of expression of the housekeeping gene β-actin).

Out of the 188 cases informative for molecular results (Table 3), 144 cases were positive for the *EWSR1* translocation. Of these, 108 cases were positive for the t(11; 22) *EWSR1-FLI1* translocation, 12 cases were positive for the *EWSR1-ERG* gene fusion, and 1 case was positive for the *EWSR1-FEV* gene fusion. The remaining 23 cases had insufficient RNA quality for RT-PCR but FISH analysis revealed the *EWSR1* rearrangement (Table 4).

Negative molecular results were obtained in 44 cases (Table 5); in these cases the *EWSR1-FLI1*, *EWSR1-ERG*, and *EWSR1-FEV* transcripts were not observed by RT-PCR technique. These same cases were also negative for the *EWSR1* and *FUS* rearrangements on FISH analysis. According to the pathologist's requests, which differed according to the various differential diagnoses, RT-PCR and/or FISH was performed on the 44 negative cases to exclude or diagnose other small round cell tumors. For synovial sarcoma, we tested for t(X;18) *SSX-SS18* (previously *SSX-SYT*) by RT-PCR and/or LSI probe for *SS18* by FISH. For rhabdomyosarcoma, we tested for t(1;13) *PAX7-FOXO1* (previously *PAX7-FKHR*) and t(2;13) *PAX3-FOXO1* by RT-PCR and/or LSI probe for *FOXO1* by FISH. For congenital fibrosarcoma, we tested for t(12;15) *ETV6-NTRK3* by RT-PCR. For desmoplastic round cell tumor, we tested for t(11;22) *EWSR1-WT1* by RT-PCR. Finally, for round cell myxoid liposarcoma, we tested for t(12;16) *DDIT3-FUS* (alias *CHOP-TLS*) and t(12;

Table 3.   Molecular Results and Diagnosis

RT-PCR/FISH	EFT	SRCT	Non-EFT/SRCT	Total cases
Positive for EWS translocation	144	0	0	144
Negative for EWS and FUS translocation	12	4	28	44
Total cases	156	4	28	188

EFT, Ewing's sarcoma family tumors; FISH, fluorescence *in situ* hybridization; SRCT, small round-cell tumors.

Table 4.   Summary of the 144 Positive Cases

Transcript variants	No. of cases detected	%
Detectable transcripts with RT-PCR (n = 121)		
EWSR1-FLI1 t(11;22) (n = 108)		
7/6 (type 1)	73	67.8
7/5 (type 2)	28	25.9
10/6 (type 3)	2	1.8
10/5 (type 4)	3	2.7
7/7	2	1.8
EWSR1-ERG t(21;22) (n = 12)		
7/13	10	83.3
7/10	1	8.3
10/10	1	8.3
EWSR1-FEV t(2;22)		
7/2	1	
FISH analysis (n = 23)		
EWSR1 rearrangement	23	
FUS rearrangement	0	
	144	

FISH, fluorescence *in situ* hybridization.

Table 5.   Summary of 44 Negative Cases

Case no.	RT-PCR t(11;22), t(21;22) t(2;22)	FISH LSI-*EWSR1* (22q12)	FISH LSI-*FUS* (16p11)	Additional Analysis
Final diagnosis: EFT (*n* = 12)				
1	Neg	Neg	Neg	IHC
2	Neg	Neg	Neg	IHC and MA
3	Neg	Neg	Neg	IHC and MA
4	Neg	Neg	Neg	IHC
5	Neg	Neg	Neg	IHC
6	Neg	Neg	Neg	IHC
7	Neg	Neg	Neg	IHC
8	Neg	Neg	Neg	IHC
9	Neg	Neg	Neg	IHC and MA
10	Neg	Neg	Neg	IHC and MA
11	Neg	Neg	Neg	IHC
12	Neg	Neg	Neg	IHC and MA
Final diagnosis: SRCT (*n* = 4)				
13	Neg	Neg	Neg	IHC and MA
14	Neg	Neg	Neg	IHC and MA
15	Neg	Neg	Neg	IHC and MA
16	Neg	Neg	Neg	IHC and MA
Final diagnosis: non-EFT/SRCT (*n* = 28)*				
17–44	Neg	Neg	Neg	IHC and MA

EFT, Ewing's sarcoma family tumors; FISH, fluorescence *in situ* hybridization; IHC, immunohistochemical analysis; LSI, locus-specific identifier (probe); MA, molecular analysis; SRCT, small round-cell tumors.
    *Non-EFT/SRCT: 7 lymphomas, 10 osteosarcomas, 1 myxoid liposarcoma, 1 synovial sarcoma, 1 malignant peripheral nerve sheath tumor, 2 undifferentiated cancers, 3 spindle cell sarcomas and 3 bone metastases from carcinoma.

22) *EWSR1-DDIT3* by RT-PCR and/or LSI probe for *DDIT3* by FISH analysis.

On the basis of the clinical, radiological, pathological, immunohistochemical, and molecular data, the 188 informative cases were ultimately diagnosed as follows. Of the 188 cases, 156 were EFTs, of which 144 (92%) had an *EWSR1* translocation and 12 (8%) did not, and 4 were undifferentiated SRCT, all negative for an *EWSR1* and *FUS* rearrangement; 28 cases were not EFT/SRCT and were subsequently diagnosed as 7 lymphomas, 10 os-

Table 6.   Summary of the 12 Translocation-Negative Cases Ultimately Diagnosed as EFT

Negative cases	Final EFT diagnosis	Age (years)	Site	RT-PCR t(11;22) t(21;22) t(2;22)	FISH LSI-*EWSR1* (22q12)	FISH LSI-*FUS* (16p11)	Additional RT-PCR analysis	Additional FISH analysis	IHC analysis
1	ES of bone	14	Vertebra	Neg	Neg	Neg			+ CD99, FLI1. − S100, LCA, TdT
2	ES of bone	34	Pelvis	Neg	Neg	Neg	Neg t(X;18)	Neg LSISS18	+ CD99, FLI1, caveolin 1. − S100, LCA, TdT, cytokeratin, EMA
3	Extraskeletal ES	40	Dorsum	Neg	Neg	Neg		Neg LSISS18	+ CD99, FLI1, caveolin 1. − LCA, TdT, S100, cytokeratin, chromogranin A, synaptophysin
4	ES of bone	45	Pelvis	Neg	Neg	Neg			+ CD99, caveolin 1. − LCA, TdT, cytokeratin, chromogranin A, synaptophysin
5	Extraskeletal ES	51	Pancreas	Neg	Neg	Neg			+ CD99, FLI1, caveolin 1. − S100, LCA, TdT
6	PNET	4	Cranium	Neg	Neg	Neg			+ FLI1, caveolin 1, chromogranin A, synaptophysin. − CD99, cytokeratin, LCA, TdT, desmin, smooth muscle actin, muscle actin, MYF4, myogenin
7	ES of bone	60	Vertebra	Neg	Neg	Neg			+ CD99, caveolin 1.
8	ES of bone	23	Pelvis	Neg	Neg	Neg			+ CD99, FLI1. − S100, LCA, TdT
9	ES of bone	7	Chest	Neg	Neg	Neg		Neg LSISS18	+ CD99, FLI1, caveolin 1. − S100, LCA, TdT
10	ES of bone	19	Tibia	Neg	Neg	Neg	Neg t(X;18), Neg t(1;13), Neg t(2;13)	Neg LSISS18, LSI-FKHR	+ CD99, FLI1. − LCA, TdT, desmin, smooth muscle actin, muscle actin, EMA, cytokeratin
11	PNET	23	Scapula	Neg	Neg	Neg			+ CD99, FLI1, caveolin 1, chromogranin A, synaptophysin. − LCA, TdT
12	ES of bone	23	Femur	Neg	Neg	Neg	Neg t(X;18) Neg t(12;16) Neg t(12;22)	Neg LSI-SS18 LSI-DDIT3	+ CD99, FLI1. − S100, LCA, TdT, smooth muscle actin, muscle actin, desmin, MYF4, myogenin

EFT, Ewing's sarcoma family tumors; EMA, epithelial membrane antigen; ES, Ewing's sarcoma; FISH, fluorescence *in situ* hybridization; IHC, immuno-histochemical analysis; LCA, leukocyte common antigen; PNET, primitive neuroectodermal tumor; TdT, terminal deoxynucleotidyl transferase; +, positive results; −, negative results.

teosarcomas, 1 myxoid liposarcoma, 1 synovial sarcoma, 1 malignant peripheral nerve sheath tumor, 2 undifferentiated cancers, 3 spindle cell sarcomas, and 3 bone metastases from carcinoma (Table 5). After molecular analysis, these 28 cases were negative for EFT translocations. The 7 lymphomas were positive for specific antibodies [leukocyte common antigen (LCA), terminal deoxynucleotidyl transferase (TdT)] after IHC analysis; moreover lymphocyte immunophenotyping confirmed lymphoma in these 7 tumors. The morphology of the 10 osteosarcomas was characterized by the production of osteoid tissue. The synovial sarcoma was positive for the *SS18-SSX* translocation (previously *SYT-SSX*) and the myxoid liposarcoma was positive for the *FUS-DDIT3* translocation (alias *TLS-CHOP*). The case ultimately diagnosed as a malignant peripheral nerve sheath tumor was positive for a specific antibody (S100 focally positive). Regarding the remaining two undifferentiated cancers and the three spindle cell sarcomas, the morphology and the IHC analysis guided the diagnosis of these entities, after excluding diagnoses on molecular analyses. The three bone metastases from carcinoma were positive for specific antibodies (cytokeratins).

The 12 cases negative for translocation that were ultimately diagnosed as EFT are summarized in Table 6. To exclude lymphoma, the IHC analysis of some specific antibodies (LCA, TdT) was performed. Out of these cases, 10 were finally diagnosed as ES (8 of bone and 2 extraskeletal), and 2 cases as PNET. Cases 1, 4, 5, 7, and 8 were diagnosed as ES because they were positive for CD99, FLI1, and/or caveolin 1 antigens and showed a classic morphology composed of sheets of monotonous round or oval cells with nuclei with smooth contours, finely dispersed chromatin, and a moderate amount of clear glycogen-rich cytoplasm. Cases 6 and 11 were diagnosed as PNET because they were positive for chromogranin and synaptophysin antigens and presented the classic Homer-Wright rosettes that are usually present in neuroectodermal tumors. Cases 2, 3, 9, 10, and 12 showed atypical morphology with poorly differentiated cells, round-to-ovoid pleomorphic nuclei, and, in some cases, appeared similar to poorly differentiated synovial sarcoma. For these cases, we performed additional molecular analyses to exclude other entities. They were negative on molecular analysis for t(X;18) and/or t(12;16), t(12;22), and/or t(1;13) or t(2;13) translocations, but were positive for CD99, FLI1, and/or caveolin 1 antigens. In these cases, the pathologist's experience allowed the final diagnosis of ES to be determined, based on IHC results, clinical features, and imaging.

Of the four cases ultimately diagnosed as SRCT, three were positive for the CD99 antigen and the remaining case was negative. Morphologically, these four tumors could have been undifferentiated ES or poorly differentiated synovial sarcoma, but the diagnosis of undifferentiated SRCT was ultimately confirmed because these tumors were negative for the t(X;18) translocation performed by RT-PCR and FISH and because the complete IHC analysis did not confirm the undifferentiated ES (CD99 was positive in three cases, but FLI1 and caveolin 1 were not). In general, the category of SRCT was assigned based on
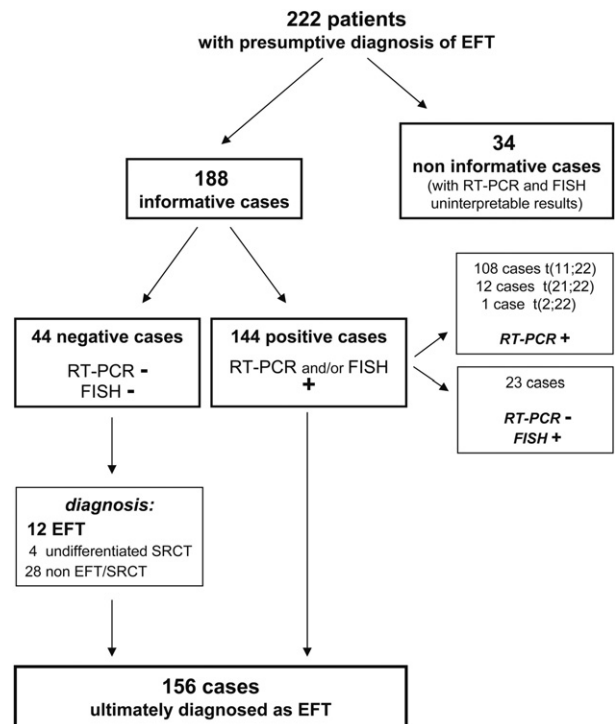

Figure 9. Schematic of results. EFT, Ewing sarcoma family tumors; FISH, fluorescence *in situ* hybridization; SRCT, small round-cell tumors; +, positive results; −, negative results.

the pathologist's experience when the morphological, antigenic, and molecular features were not diagnostic for any single established entity. All results are summarized in Figure 9 and in Tables 5 and 6.

Discussion

The gold standard for making a diagnosis of EFT is based on the complete set of clinical data, including imaging, histological, immunohistochemical, and molecular features. From a pathological point of view, the diagnosis of EFT is based on the application of specific immunohistochemical panel. The IHC panel should include vimentin, CD99, FLI1, caveolin 1, S-100, synaptophysin, chromogranin, and specific antibodies used to exclude others round cell tumors [TdT, CD45, LCA, epithelial membrane antigen (EMA), cytokeratin, desmin, actin, myogenin, MYF4]. Positivity for the CD99 antigen is a feature that is sensitive but not specific for EFT,[36,37] so it is important to test for CD99 together with other IHC markers. A further validation of the diagnosis is based on molecular analysis, because the Ewing's family of tumors is largely defined by the presence of specific translocations (because a very high percentage of these tumors are found to have the *EWSR1* rearrangement and/or *EWSR1/ETS* fusion transcripts). In the last few years, a better understanding of the molecular basis of these tumors has resulted in the greater use of molecular techniques. Molecular diagnosis, using either FISH to detect the gene rearrangement and RT-PCR to detect the fusion transcript, is now a routine part of the pathological examination of EFT[38] and has allowed for more precise diagnoses.

In the present study, we reviewed the available scientific data[3,4,7,11,12,15,16,18,24–26,33–35,39–56] to collect the most prevalent chimeric types found for EFT to date (Figures 5, 6, 7, and 8). We also report the experience of the Department of Pathology at the Rizzoli Institute from 2006 to 2009. In this 4-year period, we analyzed 222 consecutive tumors with a presumptive diagnosis of EFT; 188 cases (85%) had sufficient information for interpretation. Of these, 77% (144/188) had an *EWSR1* translocation and 23% (44/188) did not (Figure 9).

Of the tumors determined to have a translocation according to RT-PCR, 89% (108/121) had the t(11;22) *EWSR1-FLI1* translocation, and the fusion transcript *EWSR1-ERG* was found in 10% (12/121) of the cases; one case (1%) was positive for t(2;22) *EWSR1-FEV* (Table 4). FISH was performed on 23 cases in which there was insufficient RNA quality for RT-PCR or in which a translocation was not identified by RT-PCR; all 23 cases, FISH analysis revealed the *EWSR1* rearrangement. These tumors might contain rare translocations, such as t(17;22) or t(7;22) or t(20;22), that could not be detected by the primer combinations we used for RT-PCR, but that were revealed by FISH analysis. Of the remaining cases, 44/188 (23%) were negative for *EWSR1* translocations by both RT-PCR and FISH (Table 5). To evaluate whether these tumors might contain the translocations t(2;16) or t(16;21), FISH was performed for the *FUS* gene. It has been reported that, before giving a diagnosis of SRCT with a Ewing-like phenotype, it is necessary to exclude the presence of rearrangements of *FUS* as well as *EWSR1*.[40] Nonetheless, a negative molecular result should not preclude the diagnosis of EFT in the context of typical morphological, clinical, radiological, and immunophenotypic features.[7] Molecular techniques sometimes require modifications to detect rare variants,[16] and there may be variants not yet discovered. In fact, 12 cases were diagnosed as EFT even though the molecular analysis was negative (Table 6). In these cases, the pathologist's experience was critical in determining the final EFT diagnosis based on IHC results, clinical features, and radiological data, and after molecular exclusion of other entities.

In the present study, five distinct *EWSR1-FLI1* fusion transcripts were identified, representing different combinations of exons from *EWSR1* and *FLI1*. The most common was *EWSR1-FLI1* exon 7/6 fusion (type 1) (67.8%) followed by *EWSR1-FLI1* exon 7/5 fusion (type 2) (25.9%), *EWSR1-FLI1* exon 10/5 fusion (type 4) (2.7%), *EWSR1-FLI1* exon 10/6 fusion (type 3) (1.8%), and *EWSR1-FLI1* exon 7/7 fusion (1.8%). Of the 12 tumors positive for *EWSR1-ERG*, three transcript variants were found: 10 cases with *EWSR1-ERG* exon 7/13 fusion, 1 case with *EWSR1-ERG* exon 7/10 fusion, and 1 case with *EWSR1-ERG* exon 10/10 fusion.

Retrospective studies indicate a relationship between prognostic value and the specific exons involved in the translocation,[38,44,57–59] but the results are often contradictory. Prognostic relevance of the transcripts in our series was outside the scope of the present study.

Regarding IHC analysis, of the 156 tumors ultimately diagnosed as EFT, 118 cases (76%) showed moderate to strong CD99, FLI1, and/or caveolin 1 antibody positivity, whereas in 38/156 (24%) cases the CD99, FLI1, and/or caveolin 1 expression was focally inadequate for interpretation or was negative. These 38 cases were, however, positive for an *EWSR1* translocation. Previous report has confirmed the existence of CD99-negative EFT in a limited number of cases.[9] Our data reveal that IHC analysis validated 76% (118/156 cases positive for CD99, FLI1 and/or caveolin 1 with moderate to strong expression) of the cases ultimately diagnosed as EFT. This technique may, however, be limited in cases with low cellularity or uninterpretable results.

In our 4-year series, molecular analysis with RT-PCR and FISH validated approximately 92% (144/156) of the cases ultimately diagnosed as EFT. Our results are in accord with those of previous studies.[22,32]

Nonetheless, molecular techniques have their limits, as evidenced by the 15% (34/222) of cases with uninformative molecular results. Some samples were performed at different institutions, which likely have different methods of sample processing. The main problems we observed were related to fixation, excessive decalcification, and insufficient tissue. Other problems were fresh tissue kept at room temperature for too long (often in the operating room), resulting in RNA degradation. Some tissues had excessive necrosis (Bologna system 2–3)[60] induced by neoadjuvant chemotherapy.[61,62] These same problems have been also described in previous studies.[21,45]

Based on the present data, we recommend the use of both RT-PCR and FISH as complementary analyses; had we only used one or the other for each patient, the number of uninformative cases would have been higher. In our laboratory, we routinely perform RT-PCR first, because it is a rapid method and with lower costs; FISH is used secondarily whenever necessary.

In conclusion, the present study of a large series of 222 cases confirms that ancillary techniques are necessary to reach an accurate diagnosis of EFT. The optimal combination of these techniques depends on clinical and histological parameters. All three analyses (ie, IHC, RT-PCR, and FISH) are necessary in routine practice and should be performed wherever applicable, because together they provide molecular confirmation of the diagnosis of EFT.

Acknowledgments

References

1. Khoury JD: Ewing sarcoma family of tumors. Adv Anat Pathol 2005, 12:212–220
2. Llombart-Bosch A: Small round cell tumors of bone and soft tissue: introduction. Semin Diagn Pathol 1996, 13:149–152

3. Delattre O, Zucman J, Plougastel B, Desmaze C, Melot T, Peter M, Kovar H, Joubert I, de Jong P, Rouleau G, Aurias A, Thomas G: Gene fusion with an ETS DNA-binding domain caused by chromosome translocation in human tumours. Nature 1992, 359:162–165

4. Delattre O, Zucman J, Melot T, Garau XS, Zucker JM, Lenoir GM, Ambros PF, Sheer D, Turc-Carel C, Triche TJ, Aurias A, Thomas G: The Ewing family of tumors—a subgroup of small-round-cell tumors defined by specific chimeric transcripts. N Engl J Med 1994, 331: 294–299

5. O'Sullivan MJ, Perlman EJ, Furman J, Humphrey PA, Dehner LP, Pfeifer JD: Visceral primitive peripheral neuroectodermal tumors: a clinicopathologic and molecular study. Hum Pathol 2001, 32:1109–1115

6. Folpe AL, Goldblum JR, Rubin BP, Shehata BM, Liu W, Dei Tos AP, Weiss SW: Morphologic and immunophenotypic diversity in Ewing family tumors: a study of 66 genetically confirmed cases. Am J Surg Pathol 2005, 29:1025–1033

7. Pinto A, Dickman P, Parham D: Pathobiologic markers of the Ewing sarcoma family of tumors: state of the art and prediction of behaviour. Sarcoma 2011, [Epub ahead of press]

8. Ushigome S, Machinami R, Sorensen PH: Ewing sarcoma/primitive neuroectodermal tumour (PNET). Pathology and Genetics of Tumours of Soft Tissue and Bone, ed 2, ch 14. Edited by Fletcher, CDM Unni, KK Mertens. F World Health Organization Classification of Tumours 5. Lyon: IARC Press, 2002, pp 297–300

9. Llombart-Bosch A, Machado I, Navarro S, Bertoni F, Bacchini P, Alberghini M, Karzeladze A, Savelov N, Petrov S, Alvarado-Cabrero I, Mihaila D, Terrier P, Lopez-Guerrero JA, Picci P: Histological heterogeneity of Ewing's sarcoma/PNET: an immunohistochemical analysis of 415 genetically confirmed cases with clinical support. Virchows Arch 2009, 455:397–411

10. Kaneko Y, Kobayashi H, Handa M, Satake N, Maseki N: EWS-ERG fusion transcript produced by chromosomal insertion in a Ewing sarcoma. Genes Chromosomes Cancer 1997, 18:228–231

11. Peter M, Couturier J, Pacquement H, Michon J, Thomas G, Magdelenat H, Delattre O: A new member of the ETS family fused to EWS in Ewing tumors. Oncogene 1997, 14:1159–1164

12. Jeon IS, Davis JN, Braun BS, Sublett JE, Roussel MF, Denny CT, Shapiro DN: A variant Ewing's sarcoma translocation (7;22) fuses the EWS gene to the ETS gene ETV1. Oncogene 1995, 10:1229–1234

13. Urano F, Umezawa A, Yabe H, Hong W, Yoshida K, Fujinaga K, Hata J: Molecular analysis of Ewing's sarcoma: another fusion gene: EWS-E1AF, available for diagnosis. Jpn J Cancer Res 1998, 89:703–711

14. Shing DC, McMullan DJ, Roberts P, Smith K, Chin SF, Nicholson J, Tillman RM, Ramani P, Cullinane C, Coleman N: FUS/ERG gene fusions in Ewing's tumors. Cancer Res 2003, 63:4568–4576

15. Berg T, Kalsaas AH, Buechner J, Busund LT: Ewing sarcoma-peripheral neuroectodermal tumor of the kidney with a FUS-ERG fusion transcript. Cancer Genet Cytogenet 2009, 194:53–57

16. Ng TL, O'Sullivan MJ, Pallen CJ, Hayes M, Clarkson PW, Winstanley M, Sorensen PH, Nielsen TO, Horsman DE: Ewing sarcoma with novel translocation t(2;16) producing an in-frame fusion of FUS and FEV. J Mol Diagn 2007, 9:459–463

17. Szuhai K, Ijszenga M, de Jong D, Karseladze A, Tanke HJ, Hogendoorn PC: The NFATc2 gene is involved in a novel cloned translocation in a Ewing sarcoma variant that couples its function in immunology to oncology. Clin Cancer Res 2009, 15:2259–2268

18. Sumegi J, Nishio J, Nelson M, Frayer RW, Perry D, Bridge JA: A novel t(4;22)(q31;q12) produces an EWSR1-SMARCA5 fusion in extraskeletal Ewing sarcoma/primitive neuroectodermal tumor. Mod Pathol 2010, [Epub ahead of press]

19. Grier HE: The Ewing family of tumors: Ewing's sarcoma and primitive neuroectodermal tumors. Pediatr Clin North Am 1997, 44:991–1004

20. Pohar-Marinsek Z: Difficulties in diagnosing small round cell tumours of childhood from fine needle aspiration cytology samples. Cytopathology 2008, 19:67–79

21. Barr FG, Chatten J, D'Cruz CM, Wilson AE, Nauta LE, Nycum LM, Biegel JA, Womer RB: Molecular assays for chromosomal translocations in the diagnosis of pediatric soft tissue sarcomas. JAMA 1995, 273:553–557

22. Machado I, Noguera R, Pellin A, Lopez-Guerrero JA, Piqueras M, Navarro S, Llombart-Bosch A: Molecular diagnosis of Ewing sarcoma family of tumors: a comparative analysis of 560 cases with FISH and RT-PCR. Diagn Mol Pathol 2009, 18:189–199

23. Mangham DC, Williams A, McMullan DJ, McClure J, Sumathi VP, Grimer RJ, Davies AM: Ewing's sarcoma of bone: the detection of specific transcripts in a large, consecutive series of formalin-fixed, decalcified, paraffin-embedded tissue samples using the reverse transcriptase-polymerase chain reaction. Histopathology 2006, 48: 363–376

24. Qian X, Jin L, Shearer BM, Ketterling RP, Jalal SM, Lloyd RV: Molecular diagnosis of Ewing's sarcoma/primitive neuroectodermal tumor in formalin-fixed paraffin-embedded tissues by RT-PCR and fluorescence in situ hybridization. Diagn Mol Pathol 2005, 14:23–28

25. Yoshino N, Kojima T, Asami S, Motohashi S, Yoshida Y, Chin M, Shichino H, Nemoto N, Kaneko M, Mugishima H, Suzuki T: Diagnostic significance and clinical applications of chimeric genes in Ewing's sarcoma. Biol Pharm Bull 2003, 26:585–588

26. Kojima T, Asami S, Chin M, Yoshida Y, Mugishima H, Suzuki T: Detection of chimeric genes in Ewing's sarcoma and its clinical applications. Biol Pharm Bull 2002, 25:991–994

27. Sun Y, Gao D, Liu Y, Huang J, Lessnick S, Tanaka S: IGF2 is critical for tumorigenesis by synovial sarcoma oncoprotein SYT-SSX1. Oncogene 2006, 25:1042–1052

28. Antonescu CR, Elahi A, Healey JH, Brennan MF, Lui MY, Lewis J, Jhanwar SC, Woodruff JM, Ladanyi M: Monoclonality of multifocal myxoid liposarcoma: confirmation by analysis of TLS-CHOP or EWS-CHOP rearrangements. Clin Cancer Res 2000, 6:2788–2793

29. Bourgeois JM, Knezevich SR, Mathers JA, Sorensen PH: Molecular detection of the ETV6-NTRK3 gene fusion differentiates congenital fibrosarcoma from other childhood spindle cell tumors. Am J Surg Pathol 2000, 24:937–946

30. Murphy AJ, Bishop K, Pereira C, Chilton-MacNeill S, Ho M, Zielenska M, Thorner PS: A new molecular variant of desmoplastic small round cell tumor: significance of WT1 immunostaining in this entity. Hum Pathol 2008, 39:1763–1770

31. Cerveira N, Torres L, Ribeiro FR, Henrique R, Pinto A, Bizarro S, Ferreira AM, Lopes C, Teixeira MR: Multimodal genetic diagnosis of solid variant alveolar rhabdomyosarcoma. Cancer Genet Cytogenet 2005, 163:138–143

32. Gautam U, Srinivasan R, Rajwanshi A, Bansal D, Marwaha RK, Vasishtha RK: Reverse transcriptase-polymerase chain reaction as an ancillary molecular technique in the diagnosis of small blue round cell tumors by fine-needle aspiration cytology. Am J Clin Pathol 2010, 133:633–645

33. Zucman J, Melot T, Desmaze C, Ghysdael J, Plougastel B, Peter M, Zucker JM, Triche TJ, Sheer D, Turc-Carel C, Ambros P, Combaret V, Lenoir G, Aurias A, Thomas G, Delattre O: Combinatorial generation of variable fusion proteins in the Ewing family of tumours. EMBO J 1993, 12:4481–4487

34. Giovannini M, Biegel JA, Serra M, Wang JY, Wei YH, Nycum L, Emanuel BS, Evans GA: EWS-erg and EWS-Fli1 fusion transcripts in Ewing's sarcoma and primitive neuroectodermal tumors with variant translocations. J Clin Invest 1994, 94:489–496

35. Obata K, Hiraga H, Nojima T, Yoshida MC, Abe S: Molecular characterization of the genomic breakpoint junction in a t(11;22) translocation in Ewing sarcoma. Genes Chromosomes Cancer 1999, 25: 6–15

36. Ramani P, Rampling D, Link M: Immunocytochemical study of 12E7 in small round-cell tumours of childhood: an assessment of its sensitivity and specificity. Histopathology 1993, 23:557–561

37. Folpe AL, Hill CE, Parham DM, O'Shea PA, Weiss SW: Immunohistochemical detection of FLI-1 protein expression: a study of 132 round cell tumors with emphasis on CD99-positive mimics of Ewing's sarcoma/primitive neuroectodermal tumor. Am J Surg Pathol 2000, 24: 1657–1662

38. Balamuth NJ, Womer RB: Ewing's sarcoma. Lancet Oncol 2010, 11:184–192

39. Burchill SA: Ewing's sarcoma: diagnostic, prognostic, and therapeutic implications of molecular abnormalities. J Clin Pathol 2003, 56: 96–102

40. Wang L, Bhargava R, Zheng T, Wexler L, Collins MH, Roulston D, Ladanyi M: Undifferentiated small round cell sarcomas with rare EWS gene fusions: identification of a novel EWS-SP3 fusion and of additional cases with the EWS-ETV1 and EWS-FEV fusions. J Mol Diagn 2007, 9:498–509

41. Lee J, Hopcus-Niccum DJ, Mulvihill JJ, Li S: Cytogenetic and molecular cytogenetic studies of a variant of t(21;22), ins(22;21)(q12;

q21q22), with a deletion of the 3′ EWSR1 gene in a patient with Ewing sarcoma. Cancer Genet Cytogenet 2005, 159:177–180

42. Zoubek A, Pfleiderer C, Salzer-Kuntschik M, Amann G, Windhager R, Fink FM, Koscielniak E, Delattre O, Strehl S, Ambros PF, Gadner H, Kovar H: Variability of EWS chimaeric transcripts in Ewing tumours: a comparison of clinical and molecular data. Br J Cancer 1994, 70:908–913

43. Plougastel B, Zucman J, Peter M, Thomas G, Delattre O: Genomic structure of the EWS gene and its relationship to EWSR1, a site of tumor-associated chromosome translocation. Genomics 1993, 18:609–615

44. Zoubek A, Dockhorn-Dworniczak B, Delattre O, Christiansen H, Niggli F, Gatterer-Menz I, Smith TL, Jurgens H, Gadner H, Kovar H: Does expression of different EWS chimeric transcripts define clinically distinct risk groups of Ewing tumor patients? J Clin Oncol 1996, 14:1245–1251

45. Barr FG, Womer RB: Molecular diagnosis of Ewing family tumors: too many fusions? J Mol Diagn 2007, 9:437–440

46. Barr FG, Meyer WH: Role of fusion subtype in Ewing sarcoma. J Clin Oncol 2010, 28:1973–1974

47. Bhagirath T, Abe S, Nojima T, Yoshida MC: Molecular analysis of a t(11;22) translocation junction in a case of Ewing's sarcoma. Genes Chromosomes Cancer 1995, 13:126–132

48. Ida K, Kobayashi S, Taki T, Hanada R, Bessho F, Yamamori S, Sugimoto T, Ohki M, Hayashi Y: EWS-FLI-1 and EWS-ERG chimeric mRNAs in Ewing's sarcoma and primitive neuroectodermal tumor. Int J Cancer 1995, 63:500–504

49. Hisaoka M, Tsuji S, Morimitsu Y, Hashimoto H, Shimajiri S, Komiya S, Ushijima M: Molecular detection of EWS-FLI1 chimeric transcripts in Ewing family tumors by nested reverse transcription-polymerase chain reaction: application to archival paraffin-embedded tumor tissues. APMIS 1999, 107:577–584

50. Dunn T, Praissman L, Hagag N, Viola MV: ERG gene is translocated in an Ewing's sarcoma cell line. Cancer Genet Cytogenet 1994, 76:19–22

51. Selleri L, Giovannini M, Romo A, Zucman J, Delattre O, Thomas G, Evans GA: Cloning of the entire FLI1 gene, disrupted by the Ewing's sarcoma translocation breakpoint on 11q24, in a yeast artificial chromosome. Cytogenet Cell Genet 1994, 67:129–136

52. Dockhorn-Dworniczak B, Schäfer KL, Dantcheva R, Blasius S, van Valen F, Burdach S, Winkelmann W, Jürgens J, Böcker W: [Detection of EWS-/FLI-1 gene fusion transcripts by RT-PCR as a tool in the diagnosis of tumors of the Ewing sarcoma group]. German. Verh Dtsch Ges Pathol 1994, 78:214–219

53. Kovar H, Jugovic D, Melot T, Zoubek A, Lenoir G, Fink FM, Philip I, Turc-Carel C, Thomas G, Zucman-Rossi J: Cryptic exons as a source of increased diversity of Ewing tumor-associated EWS-FLI1 chimeric products. Genomics 1999, 60:371–374

54. Mastrangelo T, Modena P, Tornielli S, Bullrich F, Testi MA, Mezzelani A, Radice P, Azzarelli A, Pilotti S, Croce CM, Pierotti MA, Sozzi G: A novel zinc finger gene is fused to EWS in small round cell tumor. Oncogene 2000, 19:3799–3804

55. Noguera R, Pellin A, Navarro S, Carda C, Llombart-Bosch A: Translocation (10;11;22)(p14;q24;q12) characterized by fluorescence in situ hybridization in a case of Ewing's tumor. Diagn Mol Pathol 2001, 10:2–8

56. Sorensen PH, Triche TJ: Gene fusions encoding chimaeric transcription factors in solid tumours. Semin Cancer Biol 1996, 7:3–14

57. de Alava E, Kawai A, Healey JH, Fligman I, Meyers PA, Huvos AG, Gerald WL, Jhanwar SC, Argani P, Antonescu CR, Pardo-Mindan FJ, Ginsberg J, Womer R, Lawlor ER, Wunder J, Andrulis I, Sorensen PH, Barr FG, Ladanyi M: EWS-FLI1 fusion transcript structure is an independent determinant of prognosis in Ewing's sarcoma [Erratum appeared in J Clin Oncol 1998, 16:2895]. J Clin Oncol 1998, 16:1248–1255

58. van Doorninck JA, Ji L, Schaub B, Shimada H, Wing MR, Krailo MD, Lessnick SL, Marina N, Triche TJ, Sposto R, Womer RB, Lawlor ER: Current treatment protocols have eliminated the prognostic advantage of type 1 fusions in Ewing sarcoma: a report from the Children's Oncology Group. J Clin Oncol 2010, 28:1989–1994

59. Le Deley MC, Delattre O, Schaefer KL, Burchill SA, Koehler G, Hogendoorn PC, Lion T, Poremba C, Marandet J, Ballet S, Pierron G, Brownhill SC, Nesslböck M, Ranft A, Dirksen U, Oberlin O, Lewis IJ, Craft AW, Jürgens H, Kovar H: Impact of EWS-ETS fusion type on disease progression in Ewing's sarcoma/peripheral primitive neuroectodermal tumor: prospective results from the Cooperative Euro-E.W.I.N.G. 99 Trial. J Clin Oncol 2010, 28:1982–1988

60. Picci P, Böhling T, Bacci G, Ferrari S, Sangiorgi L, Mercuri M, Ruggieri P, Manfrini M, Ferraro A, Casadei R, Benassi MS, Mancini AF, Rosito P, Cazzola A, Barbieri E, Tienghi A, Brach del Prever A, Comandone A, Bacchini P, Bertoni F: Chemotherapy-induced tumor necrosis as a prognostic factor in localized Ewing's sarcoma of the extremities. J Clin Oncol 1997, 15:1553–1559

61. Bacci G, Ferrari S, Longhi A, Donati D, De Paolis M, Forni C, Versari M, Setola E, Briccoli A, Barbieri E: Therapy and survival after recurrence of Ewing's tumors: the Rizzoli experience in 195 patients treated with adjuvant and neoadjuvant chemotherapy from 1979 to 1997. Ann Oncol 2003, 14:1654–1659

62. Bacci G, Mercuri M, Longhi A, Bertoni F, Barbieri E, Donati D, Giacomini S, Bacchini P, Pignotti E, Forni C, Ferrari S: Neoadjuvant chemotherapy for Ewing's tumour of bone: recent experience at the Rizzoli Orthopaedic Institute. Eur J Cancer 2002, 38:2243–2251